Published in final edited form as:
Spine (Phila Pa 1976). 2012 October 1; 37(21): E1310–E1317. doi:10.1097/BRS.0b013e318267bcfc.

Seeing double: A comparison of microstructure, biomechanical function, and adjacent disc health between double-layer and single-layer vertebral endplates

Aaron J. Fields, Ph.D.[1], **Francisco Sahli Costabal, M.S.**[2], **Azucena G. Rodriguez, Ph.D.**[1], and **Jeffrey C. Lotz, Ph.D.**[1]

[1]Orthopaedic Bioengineering Laboratory, Department of Orthopaedic Surgery, University of California, San Francisco, CA, United States

[2]Department of Mechanical and Metallurgical Engineering, Pontificia Universidad Católica de Chile, Santiago, Chile

Abstract

Study design—Experimental and computational assessment of thickness, porosity, biomechanical behavior, and adjacent disc glycosaminoclycan (GAG) content in double-layer and single-layer bony endplate samples harvested from human cadaver spines.

Objective—Determine if the second layer of bone in double-layer vertebral endplates allows the superficial layer to achieve a more optimal balance between its biomechanical and nutritional functions.

Summary of background data—Proper disc health requires the endplate to balance opposing biomechanical and nutritional functions. Previous studies investigating endplate function report the occurrence of double-layer endplates, but it remains unclear whether the second layer of bone has any functional advantage. Such information could shed light on the factors that protect against disc degeneration.

Methods—Six lumbar spines were obtained from human cadavers (32–84 years) and scanned with magnetic resonance imaging. Cylindrical cores that included the endplate and underlying trabecular bone were harvested from the center of the superior vertebral endplates (six double-layer endplates and twelve single-layer endplates) and imaged using micro-CT. The thickness and porosity of the bony endplate layers was measured for each core. High-resolution finite element analysis was performed to assess biomechanical behavior. GAG content within the adjacent nucleus tissue was quantified using the dimethylmethylene blue technique.

Results—The superficial layer of the double-layer endplates was 50% thinner ($p = 0.009$) and tended also to be more porous than single-layer endplates. Strains were higher in thinner endplates; however, the second layer of bone in the double-layer endplates had a stiffening effect so that despite being thinner than single-layer endplates, the superficial layer of the double-layer endplates had a similar risk of damage. After adjusting for age, GAG content was significantly higher in the nucleus tissue adjacent to the double-layer endplates ($p = 0.01$).

Conclusion—Compared to single-layer endplates, double-layer endplates appear to permit a more optimal balance between endplate biomechanical and nutritional function and may therefore offer a significant protective factor against disc degeneration.

Corresponding author and reprint requests: Jeffrey C. Lotz, Ph.D. 513 Parnassus Avenue, S-1157, University of California, San Francisco, CA 94143-0514, United States, (415) 476-7881, fax (415) 476-1128, lotzj@orthosurg.ucsf.edu.

Keywords

disc degeneration; endplate; thickness; porosity; spine biomechanics

Introduction

Intervertebral disc degeneration is a chronic matrix remodeling process that underlies several painful disorders of the lumbar spine. Although the precise etiology of disc degeneration is unclear, with many factors being involved [1], endplate dysfunction is thought to be an important etiologic aspect of disc degeneration since the endplate plays a critical role in maintaining proper disc health [2,3]. In this study, we investigated if certain endplate phenotypes permit a more optimal balance of endplate functions and might therefore be protective against disc degeneration.

Proper disc health requires the endplate to balance opposing biomechanical and nutritional functions. Biomechanically, the endplate must be strong and resistant to damage so that it can evenly transfer load to the disc. Even minor endplate damage can disrupt the uniform distribution of disc pressure [4], and endplate damage may therefore initiate disc degeneration since abnormal pressures can inhibit disc cell metabolism [5,6] and accelerate matrix degradation [7,8]. Nutritionally, the endplate must be permeable to facilitate the inflow of glucose and oxygen to the disc cells and the outflow of lactic acid for disc matrix homeostasis [9–11]. Decreases in endplate permeability — perhaps resulting from endplate sclerosis [12,13] or cartilage damage [14] — could thus impede disc cell nutrition since the avascular disc lacks alternative nutrient pathways[15].

To understand how the endplate balances these opposing functions, a number of studies quantified the microstructure and function of single-layer vertebral endplates [12,16–20]. Anecdotally though, several studies observed a second layer of bone parallel to the superficial layer in some endplates [16,17,21,20] — one study noted the second layer in 80% of spines [16]. However, because it was difficult to reliably distinguish between the two layers of bone using sagittal sectioning, the microstructure of these ‘double-layer’ endplates has never been reported, and hence, it is unclear if the presence of the second layer of bone permits any functional advantage. With the ability to distinguish between the two layers of bone using high-resolution micro-CT imaging and to assess biomechanical function using micro-CT-based finite element analysis, we can now address this issue. Thus, in the present study we sought to quantify the microstructure and function of double-layer endplates, and thereby determine if the second layer of bone allows the superficial layer to achieve a more optimal balance between its biomechanical and nutritional functions. This study is unique since it is the first to compare the microstructure, function, and adjacent disc health between double-layer and single-layer endplates.

Materials and Methods

Cadaver materials

Six lumbar spines L2–L5 were obtained fresh-frozen from human cadavers (ages 32–84 years; one female and five males) with no medical history of musculoskeletal disorders. After thawing, all spines were scanned using MRI with an eight-channel phased-array coil and the same sagittal T2-weighted fast spin-echo sequence (GE 3T Signa Excite scanner, TE 59.36 ms, TR 4000 ms, echo train length 16, bandwidth 31.25 kHz, acquisition matrix 320 × 224, slice thickness 5 mm; GE Healthcare, Waukesha, WI). From these scans, the disc height was calculated by averaging the height measured at three midsagittal locations using standard image analysis software (NIH Image; Bethesda, MD). The spines were then

sectioned at the mid-transverse plane of each vertebra and the resulting motion segments were cored in the inferior-superior direction using a diamond coring tool (Starlite Industries; Rosemont, PA). Eighteen endplate cores (Ø-8.25 mm) from the central region of the endplates were thus obtained, each comprising one half-vertebra/disc/half-vertebra. Since the central endplate is most critical for nutrient transport to the disc nucleus [15,13], and because the superior endplates of the vertebra are more vulnerable to damage than the inferior endplates [22,23,20], we focused our study on the central region of the superior vertebral endplates and the cranially adjacent nucleus pulposus. Prior to further imaging of the cores, the disc tissue was removed and preserved for biochemistry.

Micro-CT imaging

The superior endplate cores were imaged using micro-CT with an 8-μm voxel size (μCT 40, Scanco Medical AG; Brüttisellen, Switzerland). After coarsening the images to a 16-μm voxel size, the hard tissue and marrow space were segmented using a fixed threshold value. Next, the bony endplates were identified in the scans using a custom script (IDL 8.1, Exelis Visual Information Solutions; Boulder, CO). The script uses a moving average of the thickness of the endplate to account for its porous nature and to determine the boundary between the endplate and any abutting trabeculae. For samples with double-layer endplates, a second script with a similar algorithm was used to identify the deep layer of bone after the superficial layer of bone and intervening trabeculae were removed (Figure 1).

Two microstructural parameters — porosity and thickness — were derived for each endplate. Porosity was determined as the fraction of pore volume per tissue volume in the endplate, where the tissue volume in the images was found using successive dilate and erode cycles to close and open the endplate structure. The thickness of the endplate was found by averaging the thickness calculated at each point on the cranial surface of the endplate. This thickness was defined as the distance between the cranial and caudal surfaces along the line normal to the surface at the point. In the cores with double-layer endplates, the porosity and thickness were calculated separately for the superficial and deep layers. In the cores with single-layer endplates, these parameters were calculated for the single layer.

Biochemistry

The health of the nucleus pulposus that was cranially adjacent to each endplate was determined by assessing GAG/cell and GAG content [24]. After digestion in papain for 24–36 hours, a pellet containing the cells was separated from the supernatant and re-suspended in 300 mL of buffer to estimate nucleus cell density by DNA fluorescence (Picogreen, Molecular Probes Invitrogen Detection Technologies; Eugene, OR). Fluorescence was compared to the results from a standard curve produced with known concentrations of calf thymus DNA. Cell density was calculated by assuming a constant amount of DNA per cell (6 pg/cell) [25].

Nucleus GAG content was quantified using the dimethylmethylene blue assay [26]. Briefly, the GAG content was calculated on the basis of a standard curve produced with chondroitin sulfate C (chondroitin-6 sulfate, Sigma Aldrich; St. Louis, MO). GAG content was normalized by dry weight.

Finite element modeling

To characterize the biomechanical behavior of the endplates, we performed high-resolution finite element analysis. The finite element models were created using the voxel-based technique [22,27], wherein each 16-μm cubic voxel in the coarsened scans was converted into an eight-node brick element to create a finite element model of the bony endplate and underlying trabecular bone. Element size was 10–20 times smaller than the average

thickness of the endplate and trabecular structures, thereby exceeding the minimum ratio recommended to satisfy numerical convergence criteria [28]. All bone tissue in the models was assigned the same homogeneous and isotropic material properties (E = 10 GPa, $\nu = 0.3$ [29]) since the bony endplate closely resembles a layer of fused trabeculae [18].

The cartilaginous endplate and nucleus pulposus were simulated by augmenting layers to the cranial surface of the bony endplate in the models. The height of the cartilage was chosen to match the average cartilage thickness (1.7–2.2 mm), which was measured for each endplate core using a contact micrometer. Cartilage material was modeled using properties similar to those of articular cartilage (E = 25 MPa, $\nu = 0.1$ [30]). For the nucleus pulposus, the height of the material was fixed (2.4 mm) and the properties were modeled assuming a linear relationship between the Poisson ratio and the GAG content measured for the cranially adjacent nucleus tissue (E = 8 MPa [31], ν = specimen-specific, range 0.40–0.49 [32]).

Linear finite element analysis was conducted for each model to ascertain the magnitude and distribution of the strains in the bony endplate during simulated compression. The top surface of each model (the elements representing the nucleus) was displaced in the inferior-superior direction, the magnitude of the applied displacement being 1% of the height of the model (4–6 mm). A sensitivity study indicated that the models were of sufficient height so that the strains in the bony endplate were insensitive to the boundary conditions. To provide more accurate estimates of *in situ* behavior, the strains in the outer 0.5 mm of the cores were excluded owing to the influence of a 'side-artifact' [33]. Models contained up to 35 million elements and required the use of a highly scalable, algebraic multigrid solver [34] on a massively parallel supercomputer (Sun Constellation Cluster; Texas Advanced Computing Center, Austin, TX).

The main outcome from each finite element analysis was the 90^{th} percentile limit of the maximum principal strain in the bony endplate. This value represents the tensile strain beyond which 10% of the most highly strained endplate elements were strained. This was chosen as a relative indicator of each endplate's biomechanical function since we previously found that the bone tissue belonging to the endplate has the greatest risk of initial failure overall, and that this is because of the development of high tensile strains [22]. To determine if the presence of the second, deep layer of bone altered the biomechanical efficiency of the superficial layer, we compared structure-function relationships between the superficial layer and single layer. In this case, endplate biomechanical efficiency was characterized by the (linear) relationship between the strain limit in the bony endplates and their thickness.

Statistics

We compared the microstructural parameters, biomechanical outcomes and disc health indicators between double-layer and single-layer endplates using unpaired *t*-tests (JMP 9, SAS Institute; Cary, NC). In double-layer endplates, paired *t*-tests were used to compare microstructural parameters and biomechanical outcomes between the superficial and deep layers. The effect of the second layer of bone on strain-thickness and GAG-age relationships was determined using general regression models with three explanatory variables: endplate thickness or donor age, the number of endplates (corresponds to a change in intercept), and the cross-product between thickness or donor age and the number of endplates (corresponds to a change in slope). All statistical tests were taken as significant at $p < 0.05$. Data are given as mean ± SD.

Results

Double-layer endplates were present in 2/6 spines (male donors, ages: 46 years and 66 years), and when present in a spine, they occurred at multiple levels. On T_2-weighted MRI,

double-layer endplates appeared as two sets of narrow bands that alternated between hypointense and hyperintense, whereas single-layer endplates appeared as a single set of bands that alternated between hypointense and hyperintense (Figure 2). On high-resolution micro-CT, double-layer endplates had a second, continuous layer of bone parallel to the superficial layer (Figure 1). One of the six cores with a double-layer endplate was excluded from microstructural and biomechanical analysis because it could not be analyzed using the automated script.

Microstructural analysis indicated several noteworthy differences between double-layer and single-layer endplates (Table 1). Notably, the superficial layer of the double-layer endplates was 50% thinner than the single-layer endplates. The superficial layer also tended to be more porous. Within double-layer endplates, the superficial layer was 40% thinner and over twice as porous compared to the deep layer. Qualitatively, pores in the deep layer were larger in diameter and fewer in number compared to the pores in the superficial layer (Figure 1).

Finite element analysis indicated that double-layer and single-layer endplates had similar tensile strains. Histograms comparing the frequency of the maximum principal strains between the double-layer and single-layer endplates revealed that the superficial layer and single layer had qualitatively similar strain frequencies (Figure 3A) and 90th percentile limits (266 ± 65 με *vs.* 181 ± 91 με, $p = 0.08$, Figure 3B). For all endplates, strain limits decreased significantly with increasing endplate thickness; however, the presence of the second layer of bone in the double-layer endplates had a significant effect on the slope and intercept of the structure-function relationship (Figure 4), resulting in lower strain limits for certain thicknesses than would be predicted by the relationship for single-layer endplates. In general, strains were highest at the endplates in all of the models and decreased with depth into the trabecular bone. In the models with double-layer endplates, strain limits were >80% higher in the superficial layer than in the deep layer (266 ± 65 με *vs.* 143 ± 26 με, $p = 0.003$).

Discs adjacent to double-layer endplates ($n = 6$ discs) tended to be healthier than discs adjacent to single-layer endplates ($n = 12$ discs). For all discs, GAG content ranged from 8–415 μg/mg, which is typical of nucleus pulposus tissue from lumbar discs aged 40–80 years [35]. However, while GAG content adjacent to single-layer endplates decreased significantly with age, the GAG content adjacent to single-layer endplates did not fit the same relationship, but was instead higher for a given age (Figure 5). Additionally, mean GAG/cell was significantly higher adjacent to double-layer endplates (0.018 ± 0.007 μg/cell *vs.* 0.008 ± 0.007 μg/cell, $p = 0.01$). There was no difference in disc height between double-layer and single-layer endplates (11.5 ± 2.1 mm *vs.* 9.9 ± 2.4 mm, $p = 0.18$).

Discussion

Here we present the first analysis of the microstructure and function of double-layer endplates. Our results demonstrate that compared to single-layer endplates, double-layer endplates have a thinner superficial layer and better adjacent disc health without significantly compromised biomechanical function. For single-layer endplates, thin endplates are weaker than thick endplates [36,20], and accordingly, we found that thin endplates had higher tissue strains. However, for the double-layer endplates, the presence of the second layer of bone had a stiffening effect on the superficial layer, so that the superficial layer had similar strains as the single-layer endplate — and thus, a similar risk of damage — despite being 50% thinner. Additionally, thin endplates are more permeable than thick endplates [17], and the thinner superficial layer in the double-layer endplates may therefore confer nutritional advantages to the avascular disc. Consistent with this, we found

that discs adjacent to double-layer endplates had higher nucleus pulposus GAG content and GAG/cell than did discs adjacent to single-layer endplates. The biomechanical and nutritional functions of the endplate play an important role in maintaining proper disc health [2,3]. While requiring confirmation in larger studies, our findings suggest that double-layer endplates permit a more optimal balance between these biomechanical and nutritional functions and may therefore be a significant protective factor against disc degeneration.

The endplate is the weakest link in the spinal motion segment [2,37,38], and our findings provide new insight into the dependence of endplate biomechanical behavior on its microstructure. Comparison of strain-thickness relationships between double-layer and single-layer endplates indicated that the second layer of bone enabled double-layer endplates to have a thinner superficial layer without appreciably compromising biomechanical behavior. This is because the deformations of the two layers were mechanically coupled, and thus, the second layer of bone had a stiffening effect on the superficial layer. Another aspect of endplate biomechanical behavior that may be affected by the second layer of bone is structural redundancy. Structural redundancy is an important determinant of structural fragility [39,40], and refers to the ability of the structure *e.g.* buildings and bridges, to safely redistribute load after local failure from an isolated overload. By analogy, double-layer endplates may be more structurally redundant than single-layer endplates if the second layer of bone enables load to be redistributed when the superficial layer is damaged. We explicitly tested this concept using finite element models of one double-layer and one single-layer endplate. After simulating the effects of damage to the endplate elements with strains exceeding the 90th percentile strain limit, we reloaded each of the models. Reloading the damaged endplates increased the strains in both models; however, the increase in strain was nearly 40% less for the double-layer endplate. Although preliminary, these findings suggest that double-layer endplates are more structurally redundant, and in this manner they could mitigate the accumulation of endplate damage, which is thought to accelerate disc degeneration [2] and to associate with low back pain [41].

The nutritional function of the endplate is also important for maintaining proper disc health, and our results suggest that the thinner superficial layer of double-layer endplates may facilitate nutrient transport to the disc nucleus. The vertebral capillaries that supply nutrients to the nucleus pulposus terminate at the marrow-cartilage junction [42,43,3], and direct contact between the marrow and the cartilage is a key factor that affects endplate permeability [15]. The contact area available for nutrient exchange was previously estimated to be 36% in adults [44], which is in the range of the (volumetric) porosities calculated in the present study. Importantly, endplate porosity tended to be higher in the thin, double-layer endplates than in the thick, single-layer endplates. While these trends help explain the lower GAG contents measured in the nucleus pulposus adjacent to the single-layer endplates, we caution that causality remains uncertain. For example, additional factors might also limit nutrient availability to the disc, such as reduced vertebral perfusion [45] or cartilage endplate composition [24], and thus contribute independently to variability in disc health.

Despite the potential advantages for promoting disc health, it remains unclear why double-layer endplates form. For example, we are unable to infer whether double-layer endplates are an inherited trait that is unique to some individuals or whether the feature is a remnant of endplate ossification during skeletal growth and development. In support of double-layer endplates being inherited, we offer the following evidence: 1) double-layer endplates occurred at multiple levels when they were present in a donor; 2) inherited factors account for 75% of the variability in disc degeneration [46] and these factors could result in distinct skeletal traits. Clearly, additional research is required to clarify the cause of double-layer endplates. Our findings indicate that such research may provide new insight into the factors that modify an individual's degeneration risk.

This study had several unique features compared to previous studies that quantified endplate structure and function [12,16,19,20]. Importantly, we used high-resolution micro-CT imaging and micro-CT-based finite element analysis to measure the heterogeneous endplate microstructure and to model the effects of this heterogeneity on biomechanical behavior. Further, we applied an automated software routine to systematically separate the double-layer endplates, resulting in the first comprehensive study of their distinct layers. This is beyond the capability of traditional radiological and histological approaches. A limitation of our study was the small sample size, which included only five double-layer endplates from two middle-aged donors and thus precluded a more thorough investigation of age- versus endplate-related effects on disc health. This can be addressed in future studies when additional spines with double-layer endplates become available for analysis.

In generalizing our findings, we note that our study is the only one currently available for microstructural, biomechanical, and biochemical analysis of double-layer endplates, and additional studies are therefore required to confirm these results and to extend them to a more diverse population. For single-layer endplates, our results are consistent with those of previous studies, which supports the external validity of the findings. For example, endplate thickness (0.41 ± 0.16 mm) is within the range reported by Silva *et al.* [18] (0.37 ± 0.18 mm), Edwards *et al.*[16] (0.58 ± 0.35 mm), and Zhao *et al.* [20] (0.62 ± 0.34 mm). The 90th percentile limits of the maximum principal strain (223 ± 97 με, all endplates pooled) are within the range of strains reported by previous studies using micro-CT-based finite element analysis (200–400 με [47,22,48]). Also, GAG content (range 8–415 μg/mg) is similar to measurements by Antoniou *et al.* [49] (ages 40–60 years: 356 ± 140 μg/mg; ages 60–80 years: 188 ± 117 μg/mg), and is in the lower end of the range reported by Benneker *et al.* [12] (~70–900 μg/mg), which is expected given that the disc tissue in that latter study included samples from individuals as young as 19 years. In general, the large heterogeneity in disc health— even within a single age group — signals a challenge when selecting a reference population for comparing the effects different endplate phenotypes.

It is appreciated that our analysis of endplate biomechanical function, while sophisticated, does have a number of technical limitations. The most important limitation was our focus on the central region of the superior endplates. Although this approach facilitated inter-sample comparisons, it did not account for regional variations in endplate microstructure and function [16,23,20]. A second limitation was the linear nature of the finite element models, which did not capture geometric nonlinearities such as large deformations. For example, large deformations could accentuate the stiffening effect seen in the double-layer endplates, particularly if the endplate undergoes any substantial bending. Related, the simple tissue material properties of the nucleus pulposus were intended to capture the initial behavior in response to sudden loading and do not account for material nonlinearity [50], time-dependence [51], or intra-specimen heterogeneity. Nevertheless, our conclusions regarding the relative similarity of the strain distributions between double-layer and single-layer endplates should remain valid since these limitations are thought to have a small effect on the strain distributions for this type of sudden loading compared to the overall effects of variation in endplate microstructure.

In summary, we found that double-layer endplates have a thinner superficial layer and better adjacent disc health without significantly compromised biomechanical function. Endplate function plays an important role in maintaining proper disc health. While requiring confirmation in larger studies, these findings suggest that double-layer endplates permit a more optimal balance between endplate biomechanical and nutritional functions and may therefore offer a significant protective factor against disc degeneration.

Acknowledgments

Funding Sources: National Institute of Health Grant AR052811

The manuscript submitted does not contain information about medical device(s)/drug(s). This research was supported by the National Institutes of Health (Grant AR052811), and in part by the National Science Foundation through TeraGrid resources provided by the Texas Advanced Computing Center (Grant TG-BCS110008). No benefits in any form have been or will be received from a commercial party related directly or indirectly to the subject of this manuscript.

Micro-CT and MR imaging was performed by Mr. Andrew Burghardt at the UCSF Musculoskeletal Quantitative Imaging Research Group under the direction of Dr. Sharmila Majumdar.

References

1. Buckwalter JA. Aging and degeneration of the human intervertebral disc. Spine. 1995; 20:1307–14. [PubMed: 7660243]
2. Adams MA, Freeman BJ, Morrison HP, et al. Mechanical initiation of intervertebral disc degeneration. Spine. 2000; 25:1625–36. [PubMed: 10870137]
3. Urban JP, Smith S, Fairbank JC. Nutrition of the intervertebral disc. Spine. 2004; 29:2700–9. [PubMed: 15564919]
4. Adams MA, McNally DS, Wagstaff J, et al. Abnormal stress concentrations in lumbar intervertebral discs following damage to the vertebral bodies: a cause of disc failure? Eur Spine J. 1993; 1:214–21. [PubMed: 20054920]
5. Lotz JC, Chin JR. Intervertebral disc cell death is dependent on the magnitude and duration of spinal loading. Spine. 2000; 25:1477–83. [PubMed: 10851095]
6. Walsh AJ, Lotz JC. Biological response of the intervertebral disc to dynamic loading. J Biomech. 2004; 37:329–37. [PubMed: 14757452]
7. Handa T, Ishihara H, Ohshima H, et al. Effects of hydrostatic pressure on matrix synthesis and matrix metalloproteinase production in the human lumbar intervertebral disc. Spine. 1997; 22:1085–91. [PubMed: 9160466]
8. Ishihara H, McNally DS, Urban JP, et al. Effects of hydrostatic pressure on matrix synthesis in different regions of the intervertebral disk. J Appl Physiol. 1996; 80:839–46. [PubMed: 8964745]
9. Bibby SR, Urban JP. Effect of nutrient deprivation on the viability of intervertebral disc cells. Eur Spine J. 2004; 13:695–701. [PubMed: 15048560]
10. Horner HA, Urban JP. 2001 Volvo Award Winner in Basic Science Studies: Effect of nutrient supply on the viability of cells from the nucleus pulposus of the intervertebral disc. Spine. 2001; 26:2543–9. [PubMed: 11725234]
11. Ohshima H, Urban JP. The effect of lactate and pH on proteoglycan and protein synthesis rates in the intervertebral disc. Spine. 1992; 17:1079–82. [PubMed: 1411761]
12. Benneker LM, Heini PF, Alini M, et al. 2004 Young Investigator Award Winner: vertebral endplate marrow contact channel occlusions and intervertebral disc degeneration. Spine. 2005; 30:167–73. [PubMed: 15644751]
13. Roberts S, Urban JP, Evans H, et al. Transport properties of the human cartilage endplate in relation to its composition and calcification. Spine. 1996; 21:415–20. [PubMed: 8658243]
14. Rajasekaran S, Babu JN, Arun R, et al. ISSLS prize winner: A study of diffusion in human lumbar discs: a serial magnetic resonance imaging study documenting the influence of the endplate on diffusion in normal and degenerate discs. Spine. 2004; 29:2654–67. [PubMed: 15564914]
15. Nachemson A, Lewin T, Maroudas A, et al. In vitro diffusion of dye through the end-plates and the annulus fibrosus of human lumbar inter-vertebral discs. Acta Orthop Scand. 1970; 41:589–607. [PubMed: 5516549]
16. Edwards WT, Zheng YG, Ferrara LA, et al. Structural features and thickness of the vertebral cortex in the thoracolumbar spine. Spine. 2001; 26:218–25. [PubMed: 11154545]
17. Rodriguez AG, Rodriguez-Soto AE, Burghardt AJ, et al. Morphology of the human vertebral endplate. J Orthop Res. 2011

18. Silva MJ, Wang C, Keaveny TM, et al. Direct and computed-tomography thickness measurements of the human lumbar vertebral shell and end-plate. Bone. 1994; 15:409–14. [PubMed: 7917579]
19. Wang Y, Battie MC, Boyd SK, et al. The osseous endplates in lumbar vertebrae: thickness, bone mineral density and their associations with age and disk degeneration. Bone. 2011; 48:804–9. [PubMed: 21168539]
20. Zhao FD, Pollintine P, Hole BD, et al. Vertebral fractures usually affect the cranial endplate because it is thinner and supported by less-dense trabecular bone. Bone. 2009; 44:372–9. [PubMed: 19049912]
21. Vernon-Roberts B, Pirie CJ. Degenerative changes in the intervertebral discs of the lumbar spine and their sequelae. Rheumatol Rehabil. 1977; 16:13–21. [PubMed: 847320]
22. Fields AJ, Lee GL, Keaveny TM. Mechanisms of initial endplate failure in the human vertebral body. J Biomech. 2010; 43:3126–31. [PubMed: 20817162]
23. Grant JP, Oxland TR, Dvorak MF. Mapping the structural properties of the lumbosacral vertebral endplates. Spine. 2001; 26:889–96. [PubMed: 11317111]
24. Rodriguez AG, Slichter CK, Acosta FL, et al. Human disc nucleus properties and vertebral endplate permeability. Spine. 2011; 36:512–20. [PubMed: 21240044]
25. Kim YJ, Sah RL, Doong JY, et al. Fluorometric assay of DNA in cartilage explants using Hoechst 33258. Anal Biochem. 1988; 174:168–76. [PubMed: 2464289]
26. Farndale RW, Buttle DJ, Barrett AJ. Improved quantitation and discrimination of sulphated glycosaminoglycans by use of dimethylmethylene blue. Biochim Biophys Acta. 1986; 883:173–7. [PubMed: 3091074]
27. Van Rietbergen B, Weinans H, Huiskes R, et al. A new method to determine trabecular bone elastic properties and loading using micromechanical finite element models. J Biomech. 1995; 28:69–81. [PubMed: 7852443]
28. Niebur GL, Yuen JC, Hsia AC, et al. Convergence behavior of high-resolution finite element models of trabecular bone. J Biomech Eng. 1999; 121:629–35. [PubMed: 10633264]
29. Bevill G, Eswaran SK, Farahmand F, et al. The influence of boundary conditions and loading mode on high-resolution finite element-computed trabecular tissue properties. Bone. 2009; 44:573–8. [PubMed: 19110082]
30. Athanasiou KA, Rosenwasser MP, Buckwalter JA, et al. Interspecies comparisons of in situ intrinsic mechanical properties of distal femoral cartilage. J Orthop Res. 1991; 9:330–40. [PubMed: 2010837]
31. Duncan, NA.; Lotz, JC. Computer Methods in Biomechanics and Biomedical Engineering. Vol. 527. Gordon and Breach; 1998. Experimental validation of a porohyperelastic finite element model of the annulus fibrosus.
32. Natarajan RN, Williams JR, Andersson GB. Recent advances in analytical modeling of lumbar disc degeneration. Spine. 2004; 29:2733–41. [PubMed: 15564922]
33. Bevill G, Easley SK, Keaveny TM. Side-artifact errors in yield strength and elastic modulus for human trabecular bone and their dependence on bone volume fraction and anatomic site. J Biomech. 2007; 40:3381–8. [PubMed: 17659290]
34. Adams MF, Bayraktar HH, Keaveny TM, et al. Ultrascalable implicit finite element analyses in solid mechanics with over a half a billion degrees of freedom. ACM/IEEE Proceedings of SC2004: High Performance Networking and Computing. 2004
35. Antoniou J, Steffen T, Nelson F, et al. The human lumbar intervertebral disc: evidence for changes in the biosynthesis and denaturation of the extracellular matrix with growth, maturation, ageing, and degeneration. J Clin Invest. 1996; 98:996–1003. [PubMed: 8770872]
36. Hulme PA, Boyd SK, Ferguson SJ. Regional variation in vertebral bone morphology and its contribution to vertebral fracture strength. Bone. 2007; 41:946–57. [PubMed: 17913613]
37. Brinckmann P, Frobin W, Hierholzer E, et al. Deformation of the vertebral end-plate under axial loading of the spine. Spine. 1983; 8:851–6. [PubMed: 6670020]
38. Yoganandan N, Maiman DJ, Pintar F, et al. Microtrauma in the lumbar spine: a cause of low back pain. Neurosurgery. 1988; 23:162–8. [PubMed: 2972940]
39. Feng YS, Moses F. Optimum Design, Redundancy and Reliability of Structural Systems. Computers & Structures. 1986; 24:239–51.

40. Schafer BW, Bajpai P. Stability degradation and redundancy in damaged structures. Engineering Structures. 2005; 27:1642–51.
41. Hsu KY, Zucherman JF, Derby R, et al. Painful lumbar endplate disruptions - a significant discographic finding. Spine. 1988; 13:76–8. [PubMed: 2967995]
42. Crock HV, Goldwasser M. Anatomic studies of the circulation in the region of the vertebral end-plate in adult Greyhound dogs. Spine. 1984; 9:702–6. [PubMed: 6505840]
43. Roberts S, Menage J, Urban JP. Biochemical and structural properties of the cartilage end-plate and its relation to the intervertebral disc. Spine. 1989; 14:166–74. [PubMed: 2922637]
44. Maroudas A, Stockwell RA, Nachemson A, et al. Factors involved in the nutrition of the human lumbar intervertebral disc: cellularity and diffusion of glucose in vitro. J Anat. 1975; 120:113–30. [PubMed: 1184452]
45. Liu YJ, Huang GS, Juan CJ, et al. Intervertebral disk degeneration related to reduced vertebral marrow perfusion at dynamic contrast-enhanced MRI. AJR Am J Roentgenol. 2009; 192:974–9. [PubMed: 19304703]
46. Battie MC, Videman T, Gibbons LE, et al. 1995 Volvo Award in clinical sciences. Determinants of lumbar disc degeneration. A study relating lifetime exposures and magnetic resonance imaging findings in identical twins. Spine. 1995; 20:2601–12. [PubMed: 8747238]
47. Eswaran SK, Gupta A, Keaveny TM. Locations of bone tissue at high risk of initial failure during compressive loading of the human vertebral body. Bone. 2007; 41:733–9. [PubMed: 17643362]
48. Homminga J, Van-Rietbergen B, Lochmüller EM, et al. The osteoporotic vertebral structure is well adapted to the loads of daily life, but not to infrequent “error” loads. Bone. 2004; 34:510–6. [PubMed: 15003798]
49. Antoniou J, Goudsouzian NM, Heathfield TF, et al. The human lumbar endplate. Evidence of changes in biosynthesis and denaturation of the extracellular matrix with growth, maturation, aging, and degeneration. Spine. 1996; 21:1153–61. [PubMed: 8727189]
50. Iatridis JC, Weidenbaum M, Setton LA, et al. Is the nucleus pulposus a solid or a fluid? Mechanical behaviors of the nucleus pulposus of the human intervertebral disc. Spine. 1996; 21:1174–84. [PubMed: 8727192]
51. Pollintine P, van Tunen MS, Luo J, et al. Time-dependent compressive deformation of the ageing spine: relevance to spinal stenosis. Spine. 2010; 35:386–94. [PubMed: 20110846]

Key points

1. Double-layer endplates had a thinner superficial layer than single-layer endplates.
2. Glycosaminoglycan content was higher in the nucleus pulposus adjacent to double-layer endplates than single-layer endplates.
3. Strains in the bony endplate depended on its thickness but the overall structural integrity in the double-layer and single-layer endplates was similar.
4. Compared to single-layer endplates, double-layer endplates appear to permit a more optimal balance between endplate biomechanical and nutritional function and may therefore offer a significant protective factor against disc degeneration.

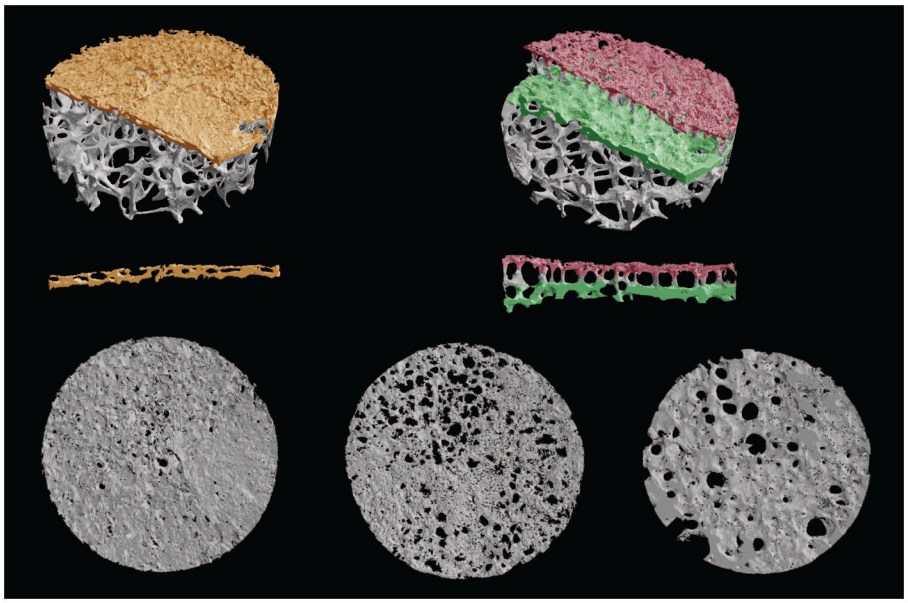

Figure 1.
μCT renderings of single-layer and double-layer bony endplate cores showing the single layer (orange and bottom left), superficial layer (red and bottom center), and deep layer (green and bottom right) identified for microstructure analysis. Cross-sections (0.5-mm-thick) through the center of the endplates illustrate the row of vertical trabeculae separating the superficial layer from the deep layer. Core diameter, 8.25 mm; spatial resolution, 16 μm.

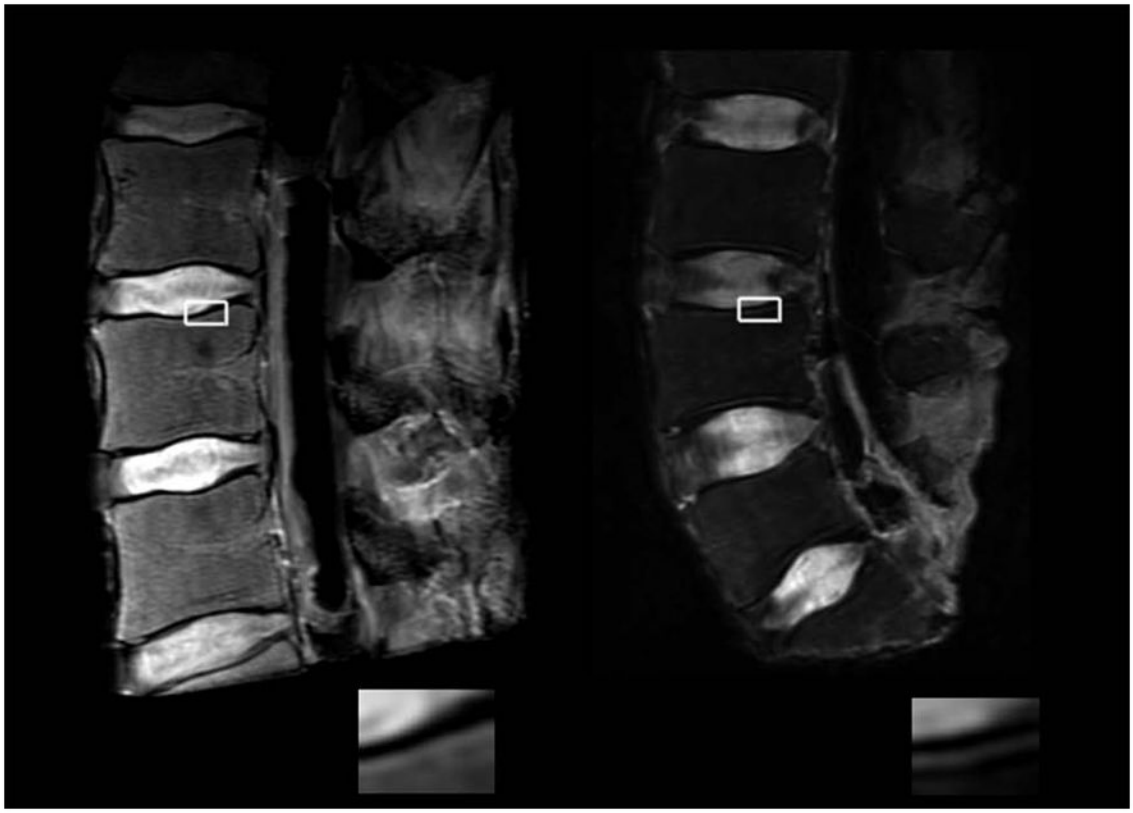

Figure 2.
Representative T_2-weighted MR images of a spine with single-layer endplates (left) and a spine with double-layer endplates (right). Spines with double-layer endplates showed two sets of bands that alternated between hypointense and hyperintense. By comparison, the endplates of spines with single-layer endplates showed the classic, single set of bands. Corresponding insets show endplate region in detail.

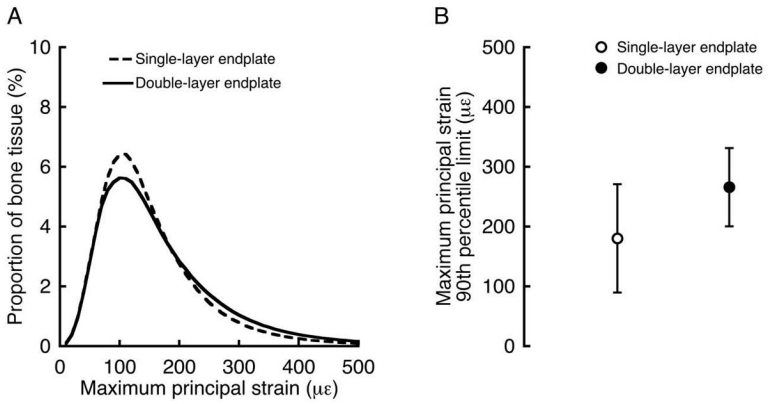

Figure 3.

(A) Histogram showing the frequency of maximum principal strains in the superficial layer of the double-layer endplates (averaged for $n = 5$ endplates) and single-layer endplates (averaged for $n = 12$ endplates). (B) Comparison of the 90th percentile limit of the maximum principal strains between the superficial layer of the double-layer endplates and single-layer endplates ($p = 0.08$).

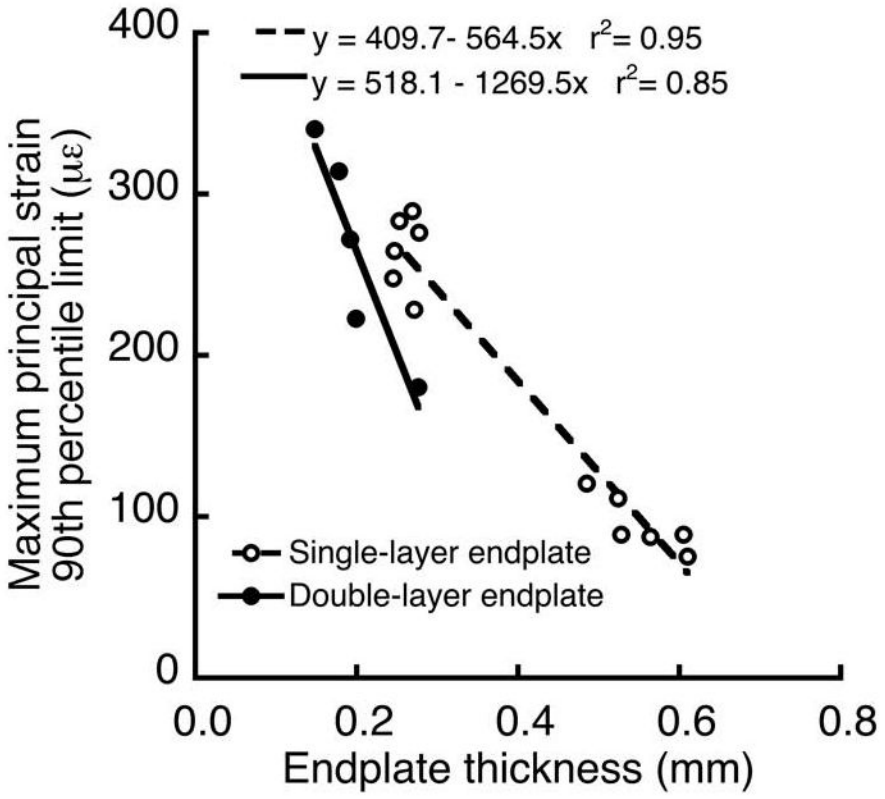

Figure 4.

The presence of the second layer of bone in the double-layer endplates had a significant effect on the relationship between the 90th percentile limit of the maximum principal strains and endplate thickness ($p = 0.01$ for differences in slope; $p = 0.003$ for differences in intercept).

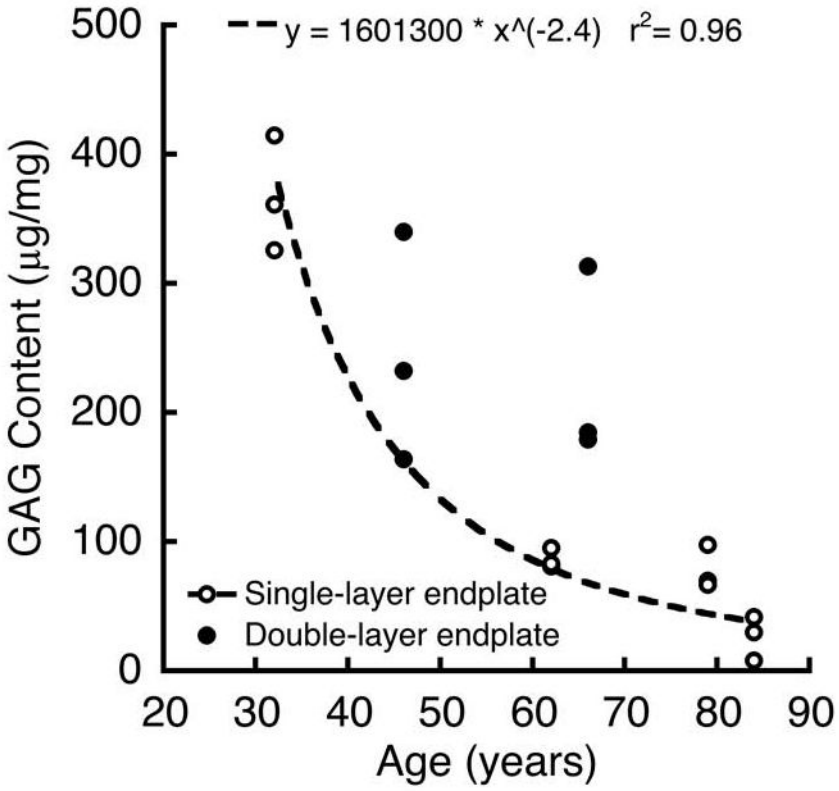

Figure 5.
Comparison between GAG-age relationships for nucleus pulposus tissue adjacent to double-layer and single-layer endplates ($p = 0.04$ for overall effect of age; $p = 0.01$ for differences in intercept; $p = 0.08$ for differences in slope).

Table 1

Comparison of bone microstructure between double-layer and single-layer endplates.

	Single-layer endplates $n = 12$	Double-layer endplates $n = 5$[c]	p-value
Endplate thickness (mm)			
Superficial layer	0.41 ± 0.16	0.19 ± 0.05	0.009[a]
Deep layer	-	0.32 ± 0.05	0.03[b]
Endplate porosity			
Superficial layer	0.29 ± 0.11	0.39 ± 0.08	0.08[a]
Deep layer	-	0.19 ± 0.05	0.003[b]
Bone volume fraction, BV/TV			
Trabecular bone	0.14 ± 0.06	0.15 ± 0.05	0.73[a]

Data given as mean ± SD.

[a] single *vs.* double, unpaired *t*-test

[b] superficial *vs.* deep, paired *t*-test

[c] one core with a double-layer endplate was excluded from microstructural analysis because it could not be analyzed using the custom script